

## Revisiting the Fresnel-phase-matched nonlinear frequency conversion

Shibin Qi <sup>1,4</sup> Ruizhi Zhao <sup>1,3</sup> Ronger Lu,<sup>1,3</sup> Jing Chen,<sup>4</sup> Xuhao Hong <sup>1,2,\*</sup> Chao Zhang,<sup>1,3,†</sup>  
Yi-Qiang Qin,<sup>1,3</sup> and Yong-Yuan Zhu<sup>1,2,‡</sup>

<sup>1</sup>National Laboratory of Solid State Microstructures, Collaborative Innovation Center of Advanced Microstructures, and Key Laboratory of Modern Acoustics, Nanjing University, Nanjing 210093, China

<sup>2</sup>School of Physics, Nanjing University, Nanjing 210093, China

<sup>3</sup>College of Engineering and Applied Sciences, Nanjing University, Nanjing 210093, China

<sup>4</sup>College of Electronic and Optical Engineering, Nanjing University of Posts and Telecommunications, Nanjing 210023, China



(Received 24 September 2019; revised 7 May 2020; accepted 27 July 2020; published 25 August 2020)

A flexible phase-matching method is introduced to manipulate the energy flow in nonlinear frequency conversion processes. With the use of photonic crystal as the reflective medium, the phase mismatching could be adjusted by the interface and the nonlinear crystal. We call this method the reflective phase matching. Here we present an experiment to demonstrate this idea in a single-domain MgO:CLN wafer with photonic crystal on the surface. A frequency-doubling signal enhanced 52 times is achieved. The result suggests the potential of the function to one more dimension phase matching without additional artificial structure inside the crystal. In addition, the proposed reflective phase-matching method could find broad application in the nonlinear optics and laser device miniaturization and integration.

DOI: [10.1103/PhysRevA.102.023529](https://doi.org/10.1103/PhysRevA.102.023529)

### I. INTRODUCTION

The development of micro- or nanostructures could break through certain scientific limitations or broaden the horizon of the physics world. Crystals, which used to be considered as high-ordered atomic structures, have special electrical and optical properties. Artificial microstructured materials such as photonic crystals (PCs), sonic crystals, or metamaterials possess unusual properties that traditional crystals do not have [1–5]. Novel optical properties such as negative refractive material, zero-index materials, superlenses, and perfect imaging could be realized in a specially designed metamaterial [6–10]. The classical Fresnel principle is challenged by the two-dimensional metasurface and has to be improved to a more generalized law [11]. In nonlinear optics, research on nonlinear photonic crystals has led us to reconsider our understanding of the conventional phenomena and concepts, for example, the nonlinear Talbot effect, the nonlinear Cerenkov effect, and nonlinear optical diffraction, to name a few [12–19]. In previous work, the Huygens principle was extended into the nonlinear regime to study local quasi-phase-matched second harmonic generation (SHG) and holographic techniques were extended to nonlinear imaging processes [20–23]. Here we combine a one-dimensional (1D) PC and a single nonlinear crystal sheet to reexamine a basic phase-matching technique which has been disregarded for a long time.

In nonlinear optics, the most famous concepts are the various kinds of phase-matching methods which have been

introduced since 1962 [24]. One of them is the so-called Fresnel phase matching (FPM) with a nonlinear crystal sheet placed in the air. The phase mismatching is compensated by the total internal reflection of all waves. Therefore, the inner reflection angle of all light should be larger than the total reflection angle in the crystal, which definitely would lead to a significant walk-off effect and severely limit the effective interaction length [25–29]. In this paper, the concept of FPM is extended to reflective phase matching (RPM) with the reflective layer replaced by a 1D PC. Thus the walk-off effect is enormously reduced. Experimentally, highly efficient second harmonic generation is realized in a MgO:CLN crystal sheet. The RPM scheme offers the possibility of miniaturization of photonic devices which might provide broad applications in nonlinear optics, laser physics, and device integration with optical multifunction.

### II. PRINCIPLES OF REFLECTIVE PHASE MATCHING

Figures 1(a) and 1(b) show the architectural design of the RPM method. A single-domain nonlinear crystal material is covered by 1D PCs as the internal reflective surfaces on both sides. The laser path, drawn in a simple line colored from red to green, reflected between the two surfaces, is zigzaglike as depicted in this figure. The fundamental wave (FW) goes through the entrance window and leaves with the generated harmonic waves from the exit window. Each wave upon each reflective surface experiences a different phase shift which is determined by the different wavelengths and the optical polarization direction.

Each zigzag length between two successive bounces ( $L$ ) depends on the thickness  $t$  of the nonlinear crystal and the reflection angle  $\beta$ , that is,  $L = t / \cos \beta$ . For the SHG interaction

\*xhhong@nju.edu.cn

†zhch@nju.edu.cn

‡yyzhu@nju.edu.cn

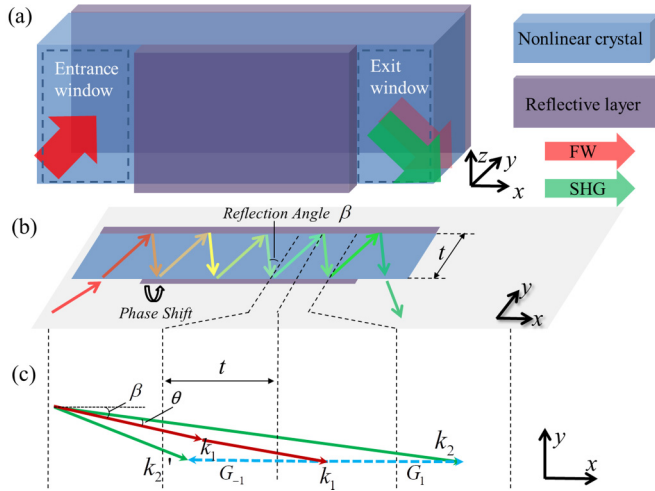


FIG. 1. Schematic diagram of (a) the RPM setup, (b) the z-axis cross section on the  $xy$  plane, and (c) the expanded view of the RPM for SHG.

in a 1D situation with the FW  $\omega_1$  and second harmonic wave frequency  $\omega_2 = 2\omega_1$ , the SHG is determined by

$$dA_2 = C\chi^{(2)}A_1^2 \exp(i\Delta kx)dx, \quad (1)$$

where  $A_1$  and  $A_2$  are the amplitudes of the FW and SHG, respectively,  $\chi^{(2)}$  is the nonlinearity coefficient of the nonlinear crystal, and  $\Delta k = k_2 - 2k_1$  stands for the wave-vector mismatching, where  $k_1$  and  $k_2$  are the wave vectors of the FW and SHG, respectively. Other coefficients, not considered in this paper, are all included in the constant  $C$ .

The global phase shift  $\Delta\Phi$  plays an important role in energy flowing in the frequency conversion process. It is considered as the sum of two major parts. The first one is the dispersion phase mismatching on propagation  $\Phi_D = \Delta kx$ . The other is the artificial relative reflective phase shift  $\Phi_R$ , which is given by  $\Phi_R = \phi_2 - 2\phi_1$ . Here  $\phi$  is the reflective phase shift of each wave. Only when the reflective phase shift  $\Phi_R$  compensates for the dispersion phase mismatching  $\Phi_D$  in each zigzag path can the energy flow continuously from the FW to the harmonic wave, that is,

$$\Delta\Phi = \Phi_D + \Phi_R = \Delta kL + \Phi_R = 2m\pi, \quad (2)$$

where  $m$  is an integer.

Assuming that the phase mismatching  $\Phi_D$  achieves  $-\pi$  before a bounce, the energy would flow back to the FW. Then an additional artificial phase shift  $\Phi_R = \pi$  is imposed into the process, which definitely results in an energy conversion, because of the presence of  $\exp(\Phi_R) = -1$ . This is equal to the function that the conventional quasi-phase-matching (QPM) method used: directly changing the crystal direction ( $\chi^{(2)} \rightarrow -\chi^{(2)}$ ) in order to obtain this minus to reverse the energy flow.

In the  $-\pi$  mismatching situation, the relationship of the output SHG amplitude to the mismatching phase and the total internal bounce time is shown in Fig. 2. It apparently indicates that the maximum SHG increases when the number of bounces is growing. In addition, the maximum output values exist under a certain condition that dispersion phase mismatching is close to the odd multiple of  $-\pi$  when the

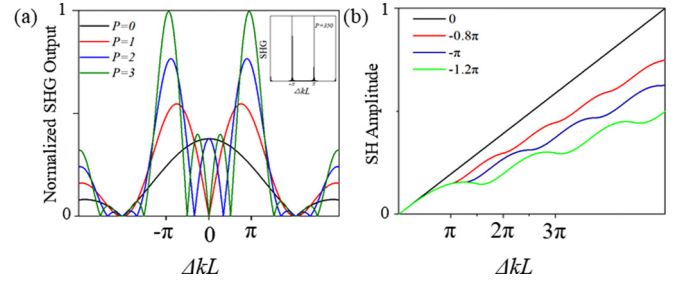


FIG. 2. (a) Calculated output SHG as a function of the phase mismatching with different total internal bounces  $P$  under the perfect reflective surface. The inset is the output SHG when  $P = 350$ . (b) SHG output under different phase-mismatching situations after RPM.

number of bounces is sufficient (see the inset of Fig. 2). Further, there is an obvious extinction phenomenon occurring at the  $2m\pi$  phase mismatching as shown in Fig. 2(a).

To directly understand the phenomenon, the entire RPM process could be described in terms of reciprocal space analysis. The zigzaglike light propagation path can be unfolded to a straight line as shown in Fig. 1(c). The red and green arrows represent FW and SHG wave vectors, respectively. The periodic reflective phase  $\Phi_R$  affects the behaviors of beams by the efficient reciprocal lattice vector, which is  $G_{\text{eff}}(m) = \pm m|\Phi_R/t|$ . Here the  $m$  ( $m = 1, 2, 3, \dots$ ) denote the orders of the structure reciprocal vectors; the vectors' relationships among them, depicted in the figure, are determined by

$$\vec{k}_2 - 2\vec{k}_1 = G_{\text{eff}}(m). \quad (3)$$

In the conventional FPM scheme, the reflection angle  $\beta$  must be larger than the total reflection angle, usually several tens of degrees. Thus some unexpected phase shift could affect the reflection angles differently for the FW and SHG beams according to the generalized laws of reflection and refraction or the nonlinear total internal reflection law [11,28]. Then the overlap area of the beams will gradually decrease, which leads to a drop in the conversion efficiency, which is the walk-off effect. In contrast, in the RPM method with a small reflection angle, the walk-off effect is mostly eliminated and the interaction of waves becomes nearly collinear.

Besides decreasing the walk-off effect and the single-domain crystal characteristic mentioned above, the most attractive potential promotion is that the PC's surfaces make it possible to realize near-perfect phase matching in the dispersion in a single-domain crystal. Figure 2(b) shows the SHG output for four different phase-mismatching situations after they are compensated respectively by RPM. The black line refers to the perfect-phase-matching (no dispersion) case in which no phase matching is needed and the efficiency is the highest. The blue line refers to the  $-\pi$  type phase-mismatching case, so the compensation phase is  $\pi$  and the output SHG growth curve is the same as for the traditional QPM situation. The other two phase-mismatching situations, shown as the green and the red curves, refer to the cases around the  $-\pi$  case. For example, when  $\Phi_D$  is  $0.8\pi$  (or  $1.2\pi$ ), the phase shift produced by 1D PCs can be designed to be  $\Phi_R = -0.8\pi$  (or  $-1.2\pi$ ) to completely compensate

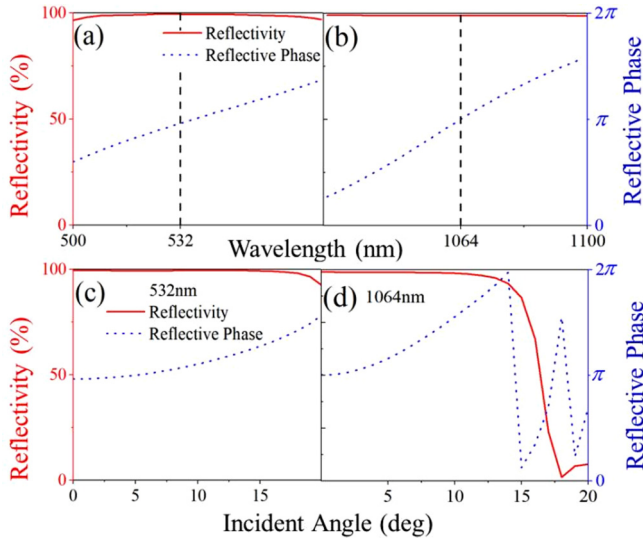


FIG. 3. Calculated reflection on the 1D PCs: the reflectivity and the reflective phase shift with wavelengths of (a) 532 nm and (b) 1064 nm under a  $0^\circ$  reflection angle. Also shown is the reflective situation of (c) SHG and (d) the FW as a function of the reflection angle.

for the dispersion phase mismatching. It is worth noting that whatever the phase mismatching  $\Phi_D$  is, there is always a compensation phase  $\Phi_R = -\Phi_D$  to match it. Thus the energy flows from the FW to SHG continuously [see Fig. 2(b)]. Theoretically, the nonlinear output in RPM has the ability to achieve a conversion efficiency as high as that for the perfect-phase-matching case.

### III. EXPERIMENTAL SETUP AND RESULTS

To demonstrate the RPM method, 1D PCs are adopted as the reflective surface on a nonlinear crystal sheet. It is well known that the 1D PCs composed of dielectric multilayer stacks with alternating refractive indices can lead to a photonic band gap and consequently provide certain reflectivity and reflective phase shift. Therefore, we adopt a common engineering film system based on periodic dielectric layer stacks of high- and low-refractive-index layers

$$(0.5H \times 0.5L)^{15}(HL)^{15}H, \quad (4)$$

where  $H$  and  $L$  represent high- and low-refractive-index layers, respectively (the structure details can be found in the Supplemental Material [30]). The free modulation of the reflective phase of the beams is realized by the complex layers on the nonlinear crystal surface. The two coating materials chosen are silicon dioxide ( $n = 1.5$ ) and hafnium oxide ( $n = 1.9$ ).

The reflectivity and reflective phase shift of the 1D PCs designed are calculated and shown in Fig. 3. The reflectivity is more than 99.5% on wavelengths of 1064 and 532 nm with a  $0^\circ$  reflection angle; it is always more than 99% around these two wavelengths. Moreover, the reflective phase shifts achieve  $\pi$  at these two wavelengths. It is worth noting that there is no obvious change in reflectivity and the reflective phase when the wavelengths shift slightly or the reflection angle is smaller than  $5^\circ$ , as can be seen in Figs. 3(c) and 3(d). These results

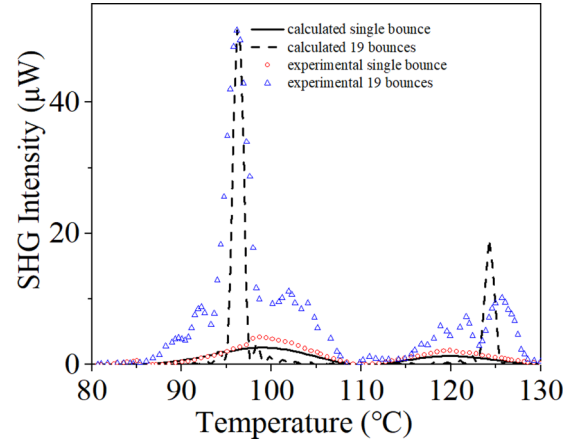


FIG. 4. Experimental and calculated results of RPM SHG with 1D PCs as the reflective surface.

provide the ability to establish a “total” internal reflection system to compensate for the phase mismatching as the FPM did, but with a smaller angle to shorten the crystal on the  $y$  axis and reduce some side effects.

In the experiment, the PCs are constructed on the  $z$  surface of a 5% mol MgO-doped lithium niobate chip (MgO:LN), which is a single domain with the same polarization direction on the whole crystal plate. The nonlinear interaction is the  $oo-e$  process, where the letters  $o$  and  $e$  represent the ordinary and the extraordinary light. The letters before the hyphen represent the polarization of the FW and that after it represents the harmonic wave. A 1064-nm continuous-wave laser such as the FW (model No. LE-LS-1064-500TA, power equal to 1.5 W, and polarization direction perpendicular to the  $z$  axis) enters a 1-mm-thick sample from the left entrance window [Fig. 1(a)]. It generates a 532-nm SHG when it propagates in a zigzag pattern in the  $xy$  plane between two reflection surfaces as shown in Fig. 1(b). Finally, the  $z$ -polarized SHG signal is collected under different temperatures from the exit window after filtering the FW. It is worth noting that the best and most direct schemes test many samples with different thicknesses. Samples with nearly the same parameters (phase shift, size of the covered PCs, etc.) except for the thickness  $t$  ( $y$  axis in Fig. 1) are not easy to fabricate. Thus we chose to tune the temperature as the same effect to change the coherent length  $L_C(2\pi/\Delta k)$ , which determines the relative propagation phase between two bounces and influences the main important relationship between the fixed zigzag length  $L$  ( $L = t/\cos\beta$ ) and  $L_C$ . Under this circumstance the SHG output can be measured at one wafer rather than testing the wafers with different physical thicknesses over and over. In order to acquire a better result, the overlap area of the beams needs to be increased. Thus the reflection angle  $\beta$  inside the crystal is controlled under  $5^\circ$  to reduce the beam walking off. Figure 4 shows the SHG intensity distribution as a function of the crystal temperature. Since  $107^\circ\text{C}$  is the birefringent phase matching (BPM) temperature of the  $oo-e$  process on MgO:LN crystal, the main peak of the direct transmission case appears at this temperature; however, in the single-bounce case (red circles in Fig. 4), the main peak splits into two peaks for which the temperature is  $96^\circ\text{C}$  or  $124^\circ\text{C}$ .

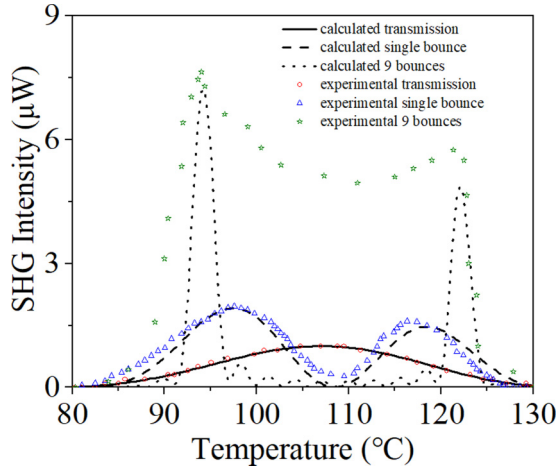


FIG. 5. Experimental and calculated results of SHG as a function of the crystal temperature based on the RPM with Ag film as the reflective surface.

The SHG distribution is extinct at  $110^\circ\text{C}$ , which is close to the BPM temperature. This situation of the peak and valley changing is similar to the case in a one-period structured crystal with two conversion domains. In addition, the peak value is nearly 4 times higher than in the direct transmission case. This means that the reflectivity is 96%, which is close to 100%. The intensity ratio of the two split peaks is 2:1, which provides a clue to deduce the actual reflection phase shift (details will be discussed later). Due to the deflection of the artificial PCs, the phase is  $0.75\pi$  rather than the ideal value  $\pi$ . The extinction effect at the BPM temperature is strong evidence that the phase shift indeed participates in the nonlinear waves coupling process. Then, in the multibounce case, the maximum SHG signal is 52 times higher than the direct transmission case when the bounces number is 19, as shown by the blue triangles in Fig. 5. The 19 bounces' zigzag path is the same as the situation of ten periods in periodically poled crystal. The results in both the single- and the multibounce cases agree well with the calculated results.

As a comparison, another sample with a simpler reflective surface is tested. Metal, especially a perfect metal, which has infinite conductivity and no loss, is the best choice of surface in RPM. Here 200 nm of Ag is evaporated on both surfaces of the MgO:LN plate. The theoretical reflectivity of Ag film is more than 96% in the spectral range considered. The phase shift on Ag should be  $0.6\pi$  at 532 nm and  $0.81\pi$  at 106 nm according to the database. Thus the total net reflective phase shift is close to  $-\pi$  ( $0.6\pi - 2 \times 0.81\pi$ ). However, in the experiment, the losses of Ag film cannot be neglected nor is the phase shift exactly equal to what we expected. The same SHG intensity distributions phenomenon is observed in the Ag surface case shown in Fig. 5. The peak value of the one-bounce case is twice that in the direct transmission case, which indicates more losses than PCs. The extinction of SHG is found at around the BPM temperature; the peak splits at a temperature of  $99^\circ\text{C}$  or  $117^\circ\text{C}$ . The maximum SHG in the nine-bounce case is 10 times higher than the direct transmission case, shown by stars in Fig. 5. Compared with

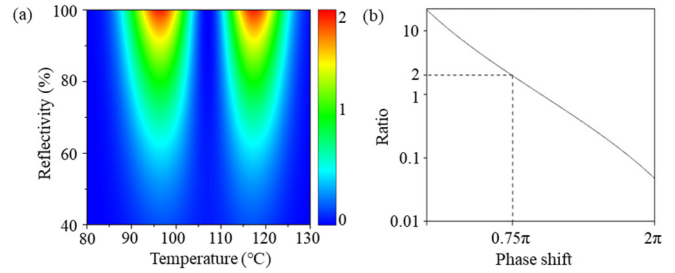


FIG. 6. (a) Calculated intensity as a function of reflectivity. (b) Ratio of two main peaks with different phase shift.

the theoretical parameter, the actual reflectivity of Ag in the experiment is 10% lower. Consequently, after several bounces both the FW and the second harmonic wave lose most of the energy and the efficient SHG output is far lower than expected.

To figure out the relationship between the nonlinear conversion and the reflection, we calculate the SHG intensity for the single-bounce situation ( $\pi$  phase shift). It is easy to understand that the output SHG becomes stronger as the reflectivity increases, which is shown in Fig. 6(a). The scale bar represents the intensity. There are always two equally split peaks because the  $\pi$  phase shift is fair enough for the two mismatching cases because whether the propagation phase shift  $\Phi_D$  goes toward  $+\pi$  ( $\Delta k > 0$ ) or  $-\pi$  ( $\Delta k < 0$ ), it can be fully compensated by the same surface reflection phase shift  $\pi$  according to the matching method [Eq. (2)]. Otherwise, the absolute values of  $\Phi_D$  are different, which causes the unequal effective efficiency of the two cases (peaks). The relationship in the one-bounce situation is calculated and shown in Fig. 6(b), which shows the phase shift determining the ratio of two peaks. Thus the ratio of 2 in the previous 1D PC experiment indicates that the phase shift on the surface is about  $0.75\pi$  [shown by the dashed line in the Fig. 6(b)].

It is universally known that in all BPM, FPM, and RPM methods, the walk-off effect is inevitable because of the noncollinear situation between the two interaction beams. The longer the propagation distance is, or the longer the reflective times are, the less energy flows from the FW to SHG due to a quick reduction of the beam overlap. Nevertheless, comparing with the other two methods, the separate angle of two waves in RPM is much smaller, which means there is more opportunity to guarantee the energy flowing positively. Therefore, in the RPM prototype, the optical nonlinear frequency conversion could achieve a high efficiency which is close to the phase-matching situation.

Another advantage of the RPM is that the mismatched phase can be compensated for and the continuous growth of the SHG can be realized in a single-domain nonlinear crystal. The folded zigzag light path has a miniaturized characteristic which could provide great opportunities for nonlinear optical system compaction and integration.

#### IV. CONCLUSION

By using a 1D PC as the reflective medium, the conventional Fresnel-phase-matching concept can be extended

to RPM. Experimentally, the maximum output SHG signal is 52 times greater than that in the phase-mismatch case in a single-domain MgO:CLN wafer. The advantage of this method can greatly reduce the walk-off effect with outstanding phase-compensating ability. Our results can be straightforwardly applied to the realization of miniaturized optical systems based on optical polarization rotation metamaterials.

## ACKNOWLEDGMENTS

This work was financially supported by the National Key Research and Development Program of China under Grant No. 2017YFA0303700; the National Natural Science Foundation of China under Grants No. 11304159, No. 11504166, No. 11874214, No. 11774165, No. 11574146, and No.11974188; and the Natural Science Foundation of Jiangsu Province under Grants No. BK20150563, No. BK20161512, and No. SBK2015042643.

- 
- [1] J. B. Pendry, A. J. Holden, W. J. Stewart, and I. Youngs, *Phys. Rev. Lett.* **76**, 4773 (1996).
- [2] R. A. Shelby, D. R. Smith, and S. Schultz, *Science* **292**, 77 (2001).
- [3] Z. Jacob, L. V. Alekseyev, and E. Narimanov, *Opt. Express* **14**, 8247 (2006).
- [4] N. Fang, H. Lee, C. Sun, and X. Zhang, *Science* **308**, 534 (2005).
- [5] C. He, S. Y. Yu, H. Ge, H. Q. Wang, Y. Tian, H. J. Zhang, X. C. Sun, Y. B. Chen, J. Zhou, M. H. Lu, and Y. F. Chen, *Nat. Commun.* **9**, 4555 (2018).
- [6] H. Suchowski, K. O'Brien, Z. J. Wong, A. Salandrino, X. B. Yin, and X. Zhang, *Science* **342**, 1223 (2013).
- [7] S. M. Wang, P. C. Wu, V. C. Su, Y. C. Lai, C. H. Chu, J. W. Chen, S. H. Lu, J. Chen, B. B. Xu, C. H. Kuan, T. Li, S. N. Zhu, and D. P. Tsai, *Nat. Commun.* **8**, 187 (2017).
- [8] G. X. Li, T. Zentgraf, and S. Zhang, *Nat. Phys.* **12**, 736 (2016).
- [9] E. Almeida, O. Bitton, and Y. Prior, *Nat. Commun.* **7**, 12533 (2016).
- [10] E. J. R. Vespeur, T. Coenen, H. Caglayan, N. Engheta, and A. Polman, *Phys. Rev. Lett.* **110**, 013902 (2013).
- [11] N. F. Yu, P. Genevet, M. A. Kats, F. Aieta, J. Tetienne, F. Capasso, and Z. Gaburro, *Science* **334**, 333 (2011).
- [12] V. Berger, *Phys. Rev. Lett.* **81**, 4136 (1998); A. Arie and N. Voloch, *Laser Photon. Rev.* **4**, 355 (2010).
- [13] N. G. R. Broderick, G.W. Ross, H. L. Offerhaus, D. J. Richardson, and D. C. Hanna, *Phys. Rev. Lett.* **84**, 4345 (2000).
- [14] S. M. Saitiel, Y. Sheng, N. Bloch, D. N. Neshev, W. Krolikowski, A. Arie, K. Koynov, and Y. S. Kivshar, *IEEE J. Quantum Electron.* **45**, 1465 (2009).
- [15] Y. Zhang, J. M. Wen, S. N. Zhu, and M. Xiao, *Phys. Rev. Lett.* **104**, 183901 (2010).
- [16] T. Ellenbogen, N. V. Bloch, A. G. Padowicz, and A. Arie, *Nat. Photon.* **3**, 395 (2009).
- [17] D. Z. Wei, C. W. Wang, H. J. Wang, X. P. Hu, D. Wei, X. Y. Fang, Y. Zhang, D. Wu, Y. L. Hu, J. W. Li, S. N. Zhu, and M. Xiao, *Nat. Photon.* **12**, 596 (2018).
- [18] N. Segal, S. Keren-Zur, N. Hendler, T. Ellenbogen, *Nat. Photon.* **9**, 180 (2015).
- [19] K. O'Brien, H. Suchowski, J. Rho, A. Salandrino, B. Kante, X. B. Yin, and X. Zhang, *Nat. Mater.* **14**, 379 (2015).
- [20] Y. Q. Qin, C. Zhang, Y. Y. Zhu, X. P. Hu, and G. Zhao, *Phys. Rev. Lett.* **100**, 063902 (2008).
- [21] X. H. Hong, B. Yang, C. Zhang, Y. Q. Qin, and Y. Y. Zhu, *Phys. Rev. Lett.* **113**, 163902 (2014).
- [22] A. Shapira, I. Juwiler, and A. Arie, *Opt. Lett.* **36**, 3015 (2011).
- [23] A. Shapira, R. Shiloh, I. Juwiler, and A. Arie, *Opt. Lett.* **37**, 2136 (2012).
- [24] J. Armstrong, N. Bloembergen, J. Ducuing, and P. Pershan, *Phys. Rev.* **127**, 1918 (1962).
- [25] G. D. Boyd and C. K. N. Patel, *Appl. Phys. Lett.* **8**, 313 (1966).
- [26] H. Komine, W. H. Long, Jr., J. W. Tully, and E. A. Stappaerts, *Opt. Lett.* **23**, 9 (1998).
- [27] R. Häïdar, P. Kupecek, E. Rosencher, R. Triboulet, and P. Lemasson, *Appl. Phys. Lett.* **82**, 1167 (2003).
- [28] M. Raybaut, A. Godard, A. Toulouse, C. Lubin, and E. Rosencher, *Opt. Express* **16**, 22 (2008).
- [29] S. Banik, S. Deb, and A. Saha, *Opt. Commun.* **287**, 196 (2013).
- [30] See Supplemental Material at <http://link.aps.org/supplemental/10.1103/PhysRevA.102.023529> for details.